Sub Topic: Diagnostics

Spring Technical Meeting
Eastern States Section of the Combustion Institute
March 10-13, 2024
Athens, Georgia

Ammonia Generation and NO_x Destruction via a Dielectric-Barrier Discharge Reactor

Joshua Landis[1,*], *Visal Veng*[1], *Yicheng Zhang*[1], *Behlol Nawaz*[1], *Md Nayer Nasim*[1], *Shubhra Kanti Das*[1], *Juan Pablo Trelles*[1], *and J. Hunter Mack*[1]

[1]*Department of Mechanical & Industrial Engineering, University of Massachusetts Lowell, One University Avenue, Lowell, Massachusetts, 01854, United States*
[*]*Corresponding Author:* joshua_landis@uml.edu

Abstract: Blends of hydrogen (H_2) and ammonia (NH_3) can potentially serve as drop-in replacements for natural gas in some power generation systems. To address adoption hurdles including the on-site generation of NH_3 and mitigation of NO_x, a dielectric-barrier discharge (DBD) reactor has been used in several different configurations. Concurrently, NO_x emissions and laminar burning velocities have been explored over a wide range of blend and equivalence ratios in a constant volume combustion chamber. The preliminary results show that the non-thermal plasma produced by the DBD reactor produces significantly more NH_3 in the presence of a catalyst and can dramatically reduce emissions of NO and NO_2.

Keywords: ***emissions, NOx control, ammonia, hydrogen, IR spectroscopy***

1. Introduction

There are several challenges associated with using neat hydrogen (H_2) as a drop-in replacement for natural gas in energy systems, including difficulties with storage and a much higher laminar burning velocity (LBV) [1]. Since NH_3 has a LBV lower than natural gas, hydrogen-ammonia (H_2-NH_3) blends have potential as a drop-in fuel for natural gas power stations with zero CO_2 emissions [2, 3]. While traditionally generated using the Haber-Bosch process, dielectric barrier discharge (DBD) plasma systems have the potential to provide distributed power stations and agricultural facilities with their own fuel and fertilizer, using ammonia produced with atmospheric nitrogen and electrolyzed water [4]. However, with the addition of H_2 to NH_3, combustion temperatures are expected to increase substantially, which can promote the generation of nitrogen oxides (NO_x) [5].

Decomposition of NO_x species is a crucial step in the replacement of natural gas with nitrogen-based hydrogen-carriers due to their considerably higher NO_x emissions compared to natural gas combustion [2]. Current methods for NO_x abatement include selective catalytic reduction (SCR) with the help of consumable NH_3 in the form of anhydrous NH_3, aqueous NH_3+H_2O, or urea. More recently, NO_x abatement has been successfully demonstrated using DBD plasma [6] in diesel and biodiesel systems without the need for consumable NH_3. The benefits of avoiding consumable NO_x create a compelling case for the use of DBD as a NO_x abatement technique for H_2-NH_3 combustion systems.

In order to quantify gas concentrations in experiments designed to both produce ammonia and destroy NO_x, IR spectroscopy can be used to sense the fundamental rotations and vibrations of the constituent gas molecules [7]. These transitions have been documented and absorb a known quantity of IR radiation at specific temperature and pressure values [8].

2. Methods/Experimental

NH_3 generation was carried out using a membrane DBD (mDBD) plasma reactor powered by high voltage alternating current arcing through a tubular membrane. This membrane is equipped with porous alumina and quartz tubes serving as dielectric barriers. Porous media used in the reactor were varied from 0.1μm, 1μm, and 2μm sized pores with a porosity of 35%, 51% and 25% respectfully. A schematic of the mDBD plasma reactor and its operating mode are shown in Figure 1.

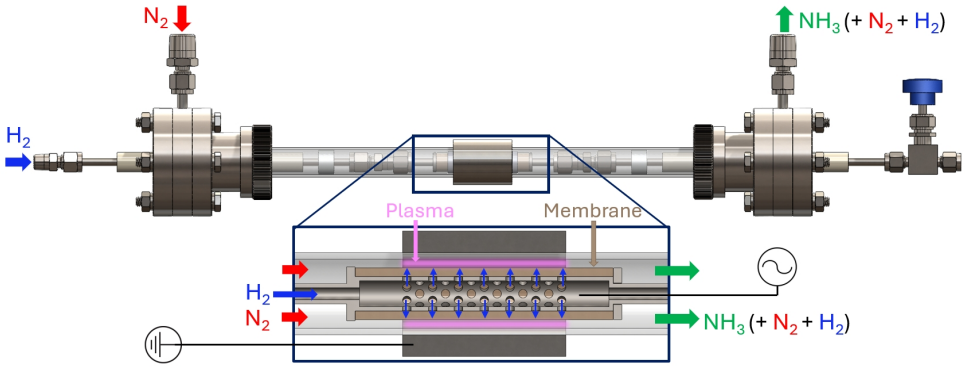

Figure 1: Design schematic of the assembled reactor with a close-up cross section of the reaction zone with porous powered electrode.

Laminar burning velocity experiments were conducted using a constant volume combustion chamber (CVCC) equipped with quartz windows to image the flame using schlieren imaging. Equivalence ratios (Φ) between 0.5 and 1.5, and H_2 fuel fractions from 0% to 50% were tested in the CVCC. A collimated light source was spanned through the optical chamber and focused onto a high-speed camera using angled parabolic mirrors. Once the reaction was ignited at the center of the chamber, this camera recorded the expanding flame and measured the propagation over time. Once combustion was complete, the resultant combustion gases were quantified using an IR spectrometer. The approach has been discussed and validated in greater detail in prior publications [9–12]. Figure 2 depicts the CVCC, gas delivery system, and data acquisition system.

NO_x decomposition was conducted using the DBD-mode of the reaction chamber similar to that seen in Figure 1, with the only difference being the lack of catalyst material and all gasses being passed through the outer passageway of the reactor. The experimental procedure consisted of flowing 912 ppm of NO and 950 ppm of NO_2 through the DBD plasma reactor at a specified flow rate. Once passed through the reactor, IR spectra was taken to measure the resulting concentration of NO_x species.

The FTIR used in each of these experiments utilized a 2 m gas cell and a deuterated triglycine sulfate (DTGS) detector. Measurements were averaged over 16 scans with a resolution of 1 cm^{-1}.

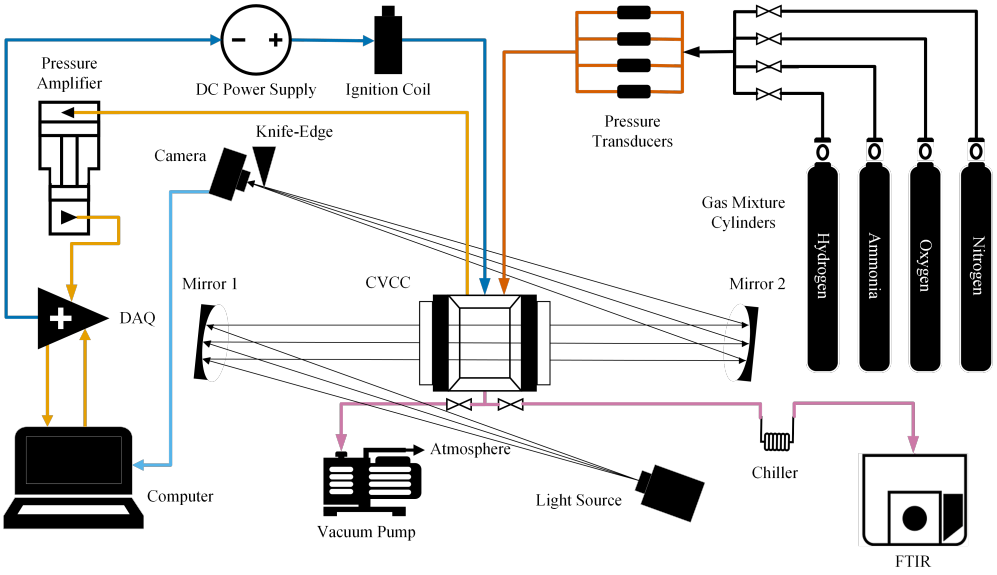

Figure 2: Schematic of the experimental setup including the CVCC coupled with Z-type Schlieren visualization, vacuum pump, ignition system, DAQ, and FTIR.

Levels of NO were measured between 1800-1870 cm^{-1} while NO_2 was measured between 1572-1644cm^{-1} and N_2O measurements were made in the 2225-2260 cm^{-1}. H_2O and NH_3 interference were mitigated through backgrounds and exhaust-gas chilling in the case of the combustion experiment.

3. Results and Discussion

IR spectra from the DBD plasma experiments showed that the highest NH_3 concentrations (1600 ppm) were attained with mDBD operation using membranes featuring 1.0 μm pore sizes and a porosity of 51% as shown in Figure 3. the maximum energy yield reached 0.35 g-NH_3/kWh. In contrast, the maximum energy yield observed under conventional DBD operation was over three times lower. This can be explained when considering the surface area of the pores is related to the diameter of each pore (assuming a relatively consistent porosity).

When the pore diameter is reduced to $\frac{1}{10}$ of its original size, we observe significant changes in the surface area. The surface area of an original pore with radius r is given by:

$$A_{\text{original}} = 2\pi rh \tag{1}$$

For a smaller pore with radius $\frac{r}{10}$, the surface area becomes:

$$A_{\text{smaller}} = 2\pi \left(\frac{r}{10}\right) h = \frac{1}{5}\pi rh \tag{2}$$

The volume of an original pore (approximated as a cylinder) is:

$$V_{\text{original}} = \pi r^2 h \tag{3}$$

The volume of a smaller pore with radius $\frac{r}{10}$ is:

$$V_{\text{smaller}} = \pi \left(\frac{r}{10}\right)^2 h = \frac{1}{100}\pi r^2 h \tag{4}$$

Since the volume of a smaller pore is $\frac{1}{100}$ the volume of an original pore, to maintain the same total volume of voids, we would need 100 times as many smaller pores. Given that each smaller pore has $\frac{1}{5}$ the surface area of a larger pore, but there are 100 times as many smaller pores, the total surface area of the smaller pores would be 20 times the total surface area of the larger pores. Therefore, the total surface area increases by a factor of 20 when the pore diameter is reduced to $\frac{1}{10}$ of its original size, assuming the porosity remains constant.

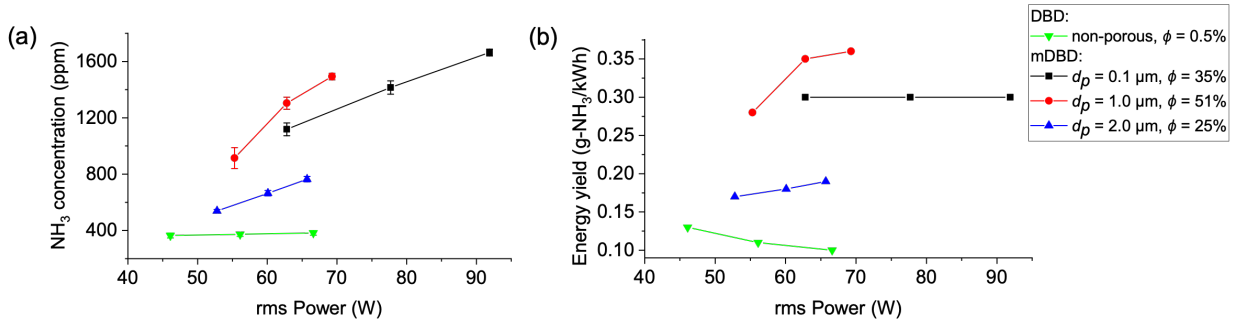

Figure 3: NH_3 concentration and energy yield of DBD and mDBD across four types of pore size and porosity and three power levels.

CVCC exhaust analysis showed a trend of NO_x being generated at a higher rate in hot, leaner flames and a deficit in rich, cooler flames. At equivalence ratios at or lower than Φ = 0.7, NO_x generation became heavily dependent on hydrogen content. N_2O formation behaves separately from NO_2 and NO emissions in that N_2O increases as conditions get leaner. As conditions get leaner, H_2 concentration plays a more vital role in the total NO_x developed up to a point whereas N_2O continues to rise. This matches recent studies showing a takeoff in N_2O production at very lean conditions [13]. Increased N_2O and decreased NO_x at Φ = 0.5-0.7 could be explained by the stability of N_2O molecules compared to NO and NO_2. N_2O is less likely to react with NH_3 as readily due to its bonds requiring significantly more energy to break compared to NO and NO_2, making it less likely to react with the unburned NH_3 in $\Phi < 0.7$ conditions [14]. Specific mechanisms for these reactions can take a variety of pathways to create N_2O and NO_x [15].

NO_x reduction by direct DBD plasma showed almost 97% of NO and 100% of NO_2 being abated from the simulated exhaust gas at 100 W. The NO_x abatement rates are shown per power input in Figure 5. Performance ceilings for 1 SLPM experiments indicate the possibility for greater emissions reductions by increasing flowrate of simulated exhaust gasses through the plasma chamber.

4. Conclusions

Potential improvements to NH_3 generation efficiency include the use of a zeolite catalyst, which has potential to amplify the abilities of a DBD reactor [16]. H_2-NH_3 blends have the potential to serve as a drop-in fuel for existing natural gas systems. While avoiding CO_2 emissions

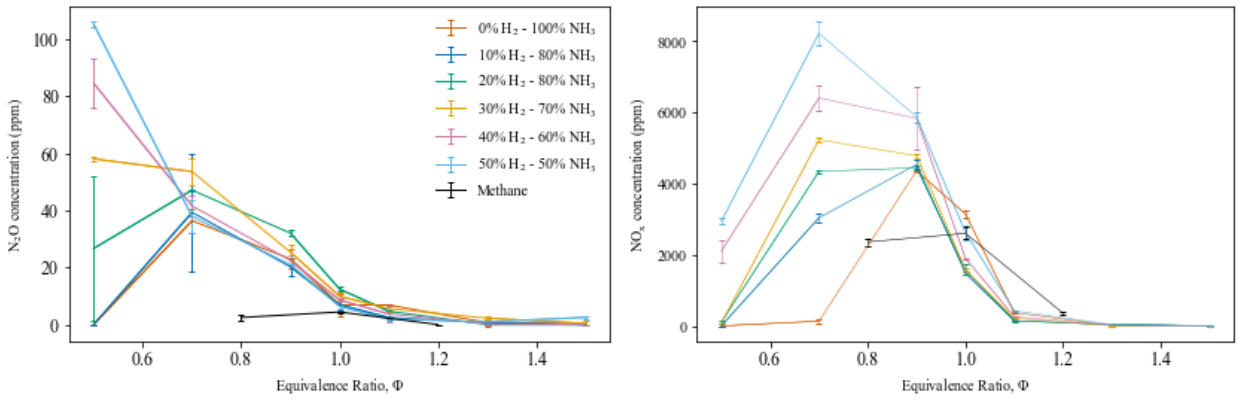

Figure 4: N_2O and NO_x emissions from CVCC Experiments compared to CH_4 combustion. Note that these figures have different vertical axis scales.

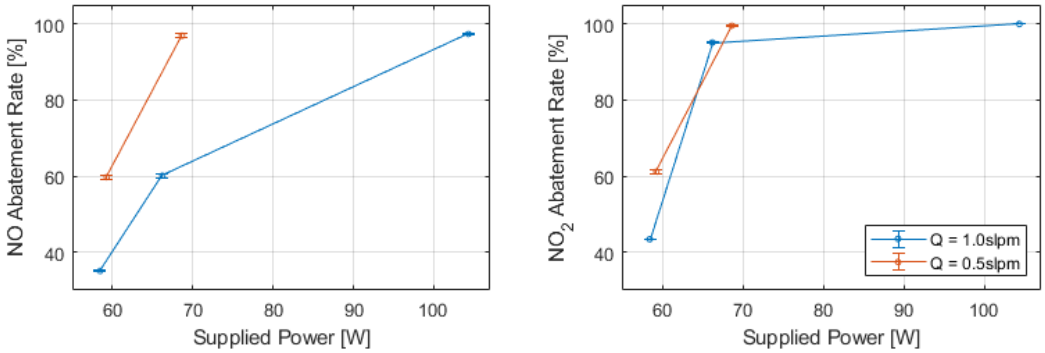

Figure 5: Steady state NO_x abatement results from DBD plasma treatment of gas mixture containing 915 ppm NO and 950 ppm NO_2 at varying power and flowrates.

is desirable, an increase in NO_x emissions must be addressed. To this, DBD plasmas are potentially an effective solution to downstream NO_x removal. The next steps for investigating viability of this technology include improving experimental apparatuses and exploring higher flow rates to replicate practical tailpipe demands for running combustion engines.

5. Acknowledgements

This work relates to DON award N00014-22-1-2001 issued by the Office of Naval Research.

References

[1] P. Chiesa, G. Lozza, and L. Mazzocchi, Using hydrogen as gas turbine fuel, J. Eng. Gas Turbines Power 127 (2005) 73–80.

[2] M. N. Nasim, B. Nawaz, S. K. Das, J. Landis, A. Shaalan, N. Van Dam, J. P. Trelles, D. Assanis, and J. H. Mack, Investigation of the Laminar Burning Velocity and Exhaust Characteristics of Methane-Ammonia-Hydrogen Ternary Blends, 87561 (2023) V001T02A005.

[3] M. H. Hasan, T. M. I. Mahlia, M. Mofijur, I. Rizwanul Fattah, F. Handayani, H. C. Ong, and A. Silitonga, A comprehensive review on the recent development of ammonia as a renewable energy carrier, Energies 14 (2021) 3732.

[4] V. Veng, B. Tabu, E. Simasiku, J. Landis, J. H. Mack, M. Carreon, and J. P. Trelles, Design and characterization of a membrane dielectric-barrier discharge reactor for ammonia synthesis, Plasma Chemistry and Plasma Processing 43 (2023) 1921–1940.

[5] B. Nawaz, M. N. Nasim, S. K. Das, J. Landis, A. SubLaban, J. P. Trelles, D. Assanis, N. Van Dam, and J. H. Mack, Combustion characteristics and emissions of nitrogen oxides (NO, NO2, N2O) from spherically expanding laminar flames of ammonia–hydrogen blends, International Journal of Hydrogen Energy 65 (2024) 164–176.

[6] P. Talebizadeh, M. Babaie, R. Brown, H. Rahimzadeh, Z. Ristovski, and M. Arai, The role of non-thermal plasma technique in NOx treatment: A review, Renewable and Sustainable Energy Reviews 40 (2014) 886–901.

[7] K. P. Horn, Exhaust Composition in a Small Internal Combustion Engine Using FTIR Spectroscopy, tech. rep. Report No., Air Force Institute of Technology, 2015.

[8] L. S. Rothman, I. E. Gordon, A. Barbe, D. C. Benner, P. F. Bernath, M. Birk, V. Boudon, L. R. Brown, A. Campargue, J.-P. Champion, et al., The HITRAN 2008 molecular spectroscopic database, Journal of Quantitative Spectroscopy and Radiative Transfer 110 (2009) 533–572.

[9] M. N. Nasim, B. Nawaz, S. K. Das, A. SubLaban, L. M. G.-C. González, J. R. Serrano, and J. H. Mack, Manipulating hydrogen oxy-combustion through carbon dioxide addition, Fuel 357 (2024) 129844.

[10] M. Morovatiyan, M. Shahsavan, J. Aguilar, M. Baghirzade, and J. H. Mack, An assessment of hydrogen addition to methane combustion with Argon as a working fluid in a constant volume combustion chamber, Combustion Science and Technology 194 (2022) 2395–2413.

[11] M. Morovatiyan, M. Shahsavan, M. Baghirzade, and J. H. Mack, Impact of syngas addition to methane on laminar burning velocity, Journal of Engineering for Gas Turbines and Power 143 (2021) 051004.

[12] M. Morovatiyan, M. Shahsavan, J. Aguilar, and J. H. Mack, Effect of argon concentration on laminar burning velocity and flame speed of hydrogen mixtures in a constant volume combustion chamber, Journal of Energy Resources Technology 143 (2021) 032301.

[13] K. P. Horn, Exhaust Composition in a Small Internal Combustion Engine Using FTIR Spectroscopy, (2015).

[14] R. Blaszczak, Nitrogen Oxides (NOx): Why and how they are controlled, Office of Air Quality Planning and Standards, U.S. Environmental Protection Agency, 1999.

[15] S. Verma, Parametric studies on N2O formation and destruction mechanisms, Energy conversion and management 43 (2002) 1737–1746.

[16] J. R. Shah, F. Gorky, J. Lucero, M. A. Carreon, and M. L. Carreon, Ammonia synthesis via atmospheric plasma catalysis: zeolite 5A, a case of study, Industrial & Engineering Chemistry Research 59 (2020) 5167–5176.